155. Radical Anion of Azuleno[5.6.7-cd]phenalene, a Failure of the Simple HMO Model

by **Fabian Gerson**[1]), **Joanna Jachimowicz**[1]) and **Christian Jutz**[2])

Physikalisch-Chemisches Institut der Universität Basel, Klingelbergstrasse 80, 4056 Basel, Switzerland, and

Organisch-Chemisches Laboratorium der Technischen Universität München, Arcisstrasse 21, 8 München 2, Germany

Herrn Prof. Dr. *Pl. A. Plattner* zum 70. Geburtstag gewidmet

(14. V. 74)

Summary. Hyperfine proton coupling constants are reported for the radical anions of azuleno-[5.6.7-*cd*]phenalene (I), 6-phenylazulene (II) and the corresponding 1,3-dideuterio-derivatives (I-d_2 and II-d_2). The singly occupied orbitals of both $I^{\ominus}$ and $II^{\ominus}$ are found to be symmetric with respect to the mirror plane perpendicular to the plane of the molecule. In the case of I, surprisingly, such an orbital corresponds not to the *first*, but to the *second* lowest antibonding HMO. A correlation diagram for the relevant orbitals of I and II indicates that the correct energy order in the HMO model of I can be achieved by a decrease in the absolute value of the parameter $\beta_{\mu\nu}$ for the bonds 4a–5, 6–6a, 9a–10 and 11–11a.

The simple HMO model (in which the parameters α_μ and $\beta_{\mu\nu}$ are not modified relative to their standards α and β) has been successfully used to reproduce or predict the π-spin distributions in the radical ions of aromatic hydrocarbons. Although the HMO spin populations require further refinement, which should account for π–π spin polarization, good agreement has been found between the HMO theoretical values and the experimental data as determined by ESR. spectroscopy [1]. This agreement implies that the HMO chosen as the singly occupied orbital of the radical ion possesses the proper nodal properties. The gratifying experience that such a choice has always been adequate is due to the 'correct' sequence of the HMO's in the relevant energy region. Correct signifies that the top filled HMO (in general, the highest bonding one) and the bottom vacant HMO of the π-system (in general, the lowest antibonding one) have the same symmetry as the singly occupied orbital of the radical cation and the radical anion, respectively.

Nevertheless, despite the success experienced in the past, the correct energy sequence of the HMO's need not be taken for granted. Two cases should be considered. In the first case, the energy sequence is correctly given by the simple HMO model for the neutral system, but this sequence undergoes a reversal on passing from the diamagnetic compound to its radical ion. However, since such a reversal usually arises from substantial changes in geometry, it is unlikely to occur for aromatic hydrocarbons with large π-systems. In the second, more probable case, the simple HMO model fails to reflect the energy sequence even in the neutral compound. It can be anticipated that the latter case is likely to be encountered with extended nonalternant

[1]) Universität Basel.
[2]) Universität München.

π-systems which exhibit energetically close orbitals along with substantial variations in π-charge and/or bond-order. This point will be illustrated in the present paper by ESR. studies of the radical anion of azuleno[5.6.7-*cd*]phenalene (I). In addition, ESR. spectra of the radical anions of 1,3-dideuterio-azuleno[5.6.7-*cd*]phenalene (I-d_2), 6-phenylazulene (II) and 1,3-dideuterio-6-phenylazulene (II-d_2) will be described.

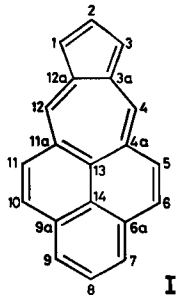

I

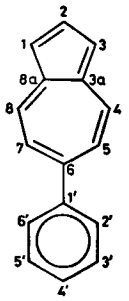

II

Experimental Part. – The syntheses of azuleno[5.6.7-*cd*]phenalene (I) and 6-phenylazulene (II) have been reported elsewhere [2] [3]. The 1,3-dideuterio-derivatives I-d_2 and II-d_2 were prepared from the respective parent hydrocarbons by isotope exchange in 85 percent D_3PO_4 (*Merck*, Darmstadt). The mass spectra confirmed the dideuteration which is known to be restricted to the 1,3-positions of I [2] [4] and II [3] [5] under the applied conditions.

The radical anions $I^{\ominus}$, I-$d_2^{\ominus}$, $II^{\ominus}$ and II-$d_2^{\ominus}$ were produced from the respective neutral compounds with potassium in 1,2-dimethoxyethane (DME). The stability of the radical anions was rather low at temperatures above $-10°$, as indicated by a decrease in the intensity of the ESR. spectra. Moreover, in the case of I and I-d_2, care had to be exercised not to push the reduction too far, since the radical anions $I^{\ominus}$ and I-$d_2^{\ominus}$ (green colour) were rapidly transformed into the respective dianions $I^{2\ominus}$ and I-$d_2^{2\ominus}$ (red colour). The rate of dianion formation was greatly enhanced when DME had been replaced by 2-methyltetrahydrofuran (MTHF) as a solvent. The frozen solutions of $I^{2\ominus}$ and I-$d_2^{2\ominus}$ in MTHF did not exhibit an ESR. absorption.

ESR. Spectra. Figures 1 to 4 show the ESR. spectra taken of the radical anions $I^{\ominus}$, I-$d_2^{\ominus}$, $II^{\ominus}$ and II-$d_2^{\ominus}$ at $-70°$. The accuracy achieved in the analysis of their hyperfine structures is reflected by the computer simulated *Lorentzian* curves which are reproduced below the experimental spectra.

The agreement is remarkable in view of seven different coupling constants due to the five proton pairs and the two single protons in both $I^{\ominus}$ and $II^{\ominus}$. Replacement of the 1,3-proton pair by two deuterons to yield I-$d_2^{\ominus}$ and II-$d_2^{\ominus}$, respectively, led to an effective decrease in this number from seven to six, since the deuteron hyperfine splittings were too small to be resolved and solely gave rise to enhanced line-widths (*cf.* footnote g to the Table and legends to Fig. 2 and 4). It is noteworthy that in the simulation precisely the same values were used for the six proton coupling constants common to the radical anions of parent and dideuterated compounds.

The Table lists the pertinent coupling constants $a_{H\mu}$. A partial assignment of these values, which is sufficient for an unequivocal symmetry characterization of the singly occupied orbitals, results from experiment. The residual assignment is based on comparison with the analogous data for the radical anion of azulene (III) [6–8] and on MO theoretical calculations. The values $a_{H\mu}$ for $III^{\ominus}$ and the calculated π-spin populations ϱ_μ for $I^{\ominus}$, $II^{\ominus}$ and $III^{\ominus}$ are also included in the Table; the MO models underlying these numbers ϱ_μ will be dealt with in the Discussion.

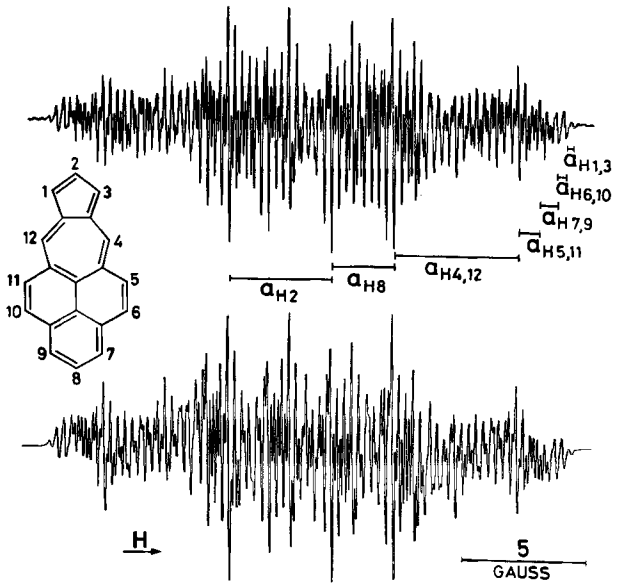

Fig. 1. *ESR. spectra of the radical anion* $I^{\ominus}$. Top: Experimental spectrum. Solvent: DME; counterion: $K^{\oplus}$; temp.: $-70°$. Bottom: Computer simulated spectrum. Coupling constants given in the Table; line-width: 0.09 gauss; line form: *Lorentzian*

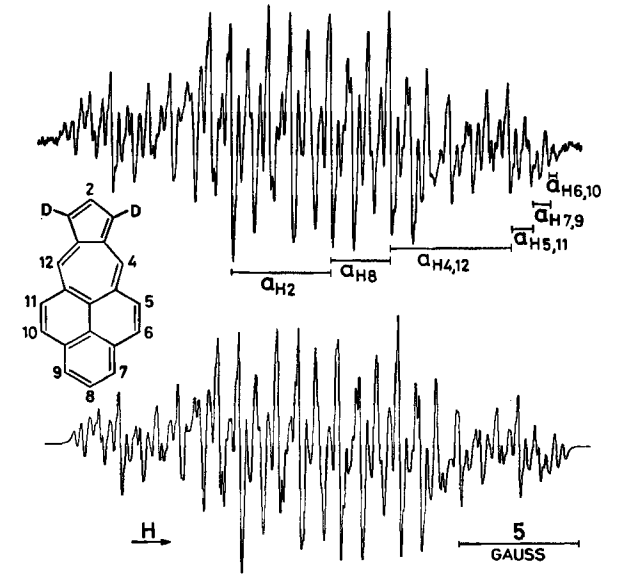

Fig. 2. *ESR. spectra of the radical anion* $I\text{-}d_2^{\ominus}$. Top: Experimental spectrum. Solvent DME; counterion: $K^{\oplus}$; temp.: $-70°$. Bottom: Computer simulated spectrum. The same coupling constants used as for $I^{\ominus}$, except $a_{H_{1,3}}$ which has been omitted; line-width: 0.15 gauss; line-shape: *Lorentzian*

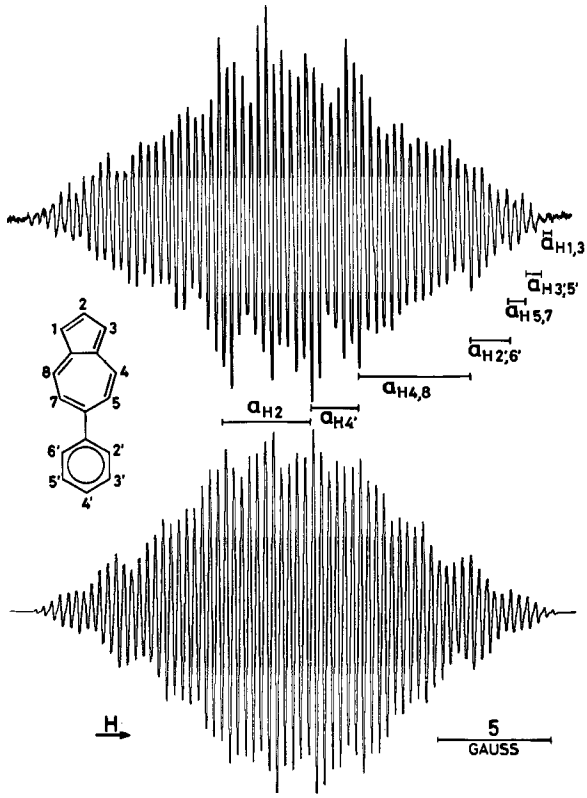

Fig. 3. *ESR. spectra of the radical anion II*$^{\ominus}$. Top: Experimental spectrum. Solvent DME; counter-ion: $K^{\oplus}$; temp.: $-70°$. Bottom: Computer simulated spectrum. Coupling constants given in the Table; line-width: 0.08 gauss; line-form: *Lorentzian*

Raising the temperature from -70 to $-10°$ had only a negligible effect on the spectra of $I^{\ominus}$ and I-$d_2^{\ominus}$. For $II^{\ominus}$, on the other hand, some reversible changes in the hyperfine pattern were observed upon variation of the temperature in this range. These changes, which have not been studied in detail, are presumably slight. Such a conclusion is supported by the finding that no marked temperature dependence was displayed by the spectrum of II-$d_2^{\ominus}$. Evidently, the corresponding changes are masked here by the substantially larger line-width.

Discussion. – Figure 5 presents schematically the two lowest antibonding HMO's, ψ_S and ψ_A of azuleno[5.6.7-*cd*]phenalene (I; symmetry group C_{2v}). They are classified as symmetric (S) or antisymmetric (A) with respect to the mirror plane which passes through the centres 2, 13, 14 and 8, and which is perpendicular to the plane of the molecule. Inspection of the experimental data $a_{H\mu}$ listed in the Table leaves no doubt that the singly occupied orbital of $I^{\ominus}$ corresponds to ψ_S and not to ψ_A (relatively large coupling constants from the protons at the centres 2 and 8, and very small ones from those at 1 and 3). This result is surprising insofar as the simple model predicts the

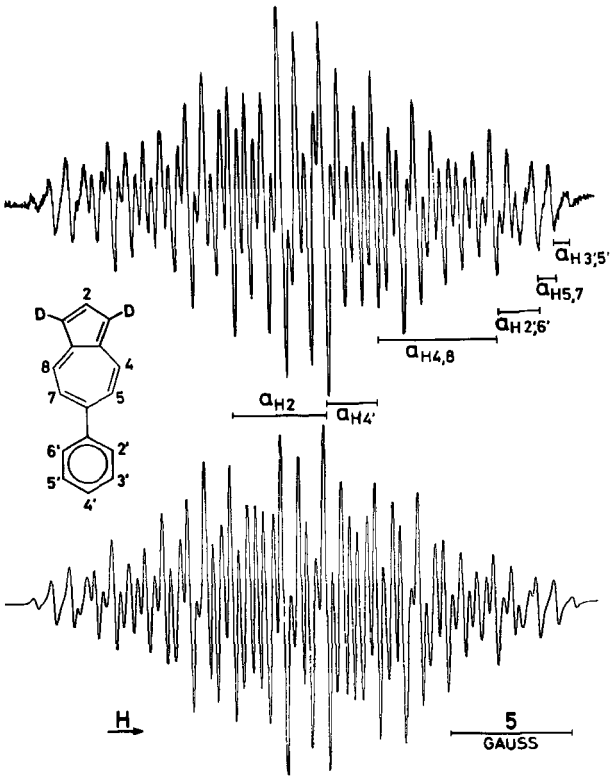

Fig. 4. *ESR. spectra of the radical anion II-$d_2^{\ominus}$.* Top: Experimental spectrum. Solvent DME; counterion: $K^{\oplus}$; temp.: −70°. Bottom: Computer simulated spectrum. The same coupling constants used as for $II^{\ominus}$, except $a_{H_{1,3}}$ which has been omitted; line-width: 0.19 gauss; line-shape: *Lorentzian*

'symmetric' HMO ψ_S to lie energetically ***higher*** than its 'antisymmetric' counterpart ψ_A.

Figure 5 also depicts the two lowest antibonding HMO's ψ_S and ψ_A of 6-phenylazulene (II; group C_{2v}) which exhibit the same symmetry behaviour as the equally labelled HMO's of I. Again, the values a_{H_μ} given in the Table clearly establish that the singly occupied orbital of $II^{\ominus}$ corresponds to the symmetric HMO ψ_S which lies here well below its antisymmetric counterpart ψ_A. Therefore, in this case, the two lowest antibonding HMO's follow the correct energy sequence which is usually found for aromatic hydrocarbons. For the considerations below, it is essential that the singly occupied orbitals of $I^{\ominus}$ and $II^{\ominus}$ belong to the same symmetry species.

The correlation diagram for the HMO's ψ_S and ψ_A of I and II is shown in Figure 6 where the pertinent energies $E = \alpha + x\beta$ are plotted vs. the parameter $\beta_{\mu\nu} = k\beta$ of the bonds $\mu - \nu$ = 4a–5, 6–6a, 9a–10 and 11–11a in I; the energies of ψ_S and ψ_A at $k = 0$ thus represent those for II. The curves cross at $k \approx 0.94$ if the parameters $\beta_{\mu\nu}$ are left equal to β for all remaining bonds (solid lines), or at $k \approx 0.86$ if $\beta_{\mu\nu}$ is taken as 0.8β for the bond 3a–12a which corresponds to the 'long' bond 3a–8a in azulene

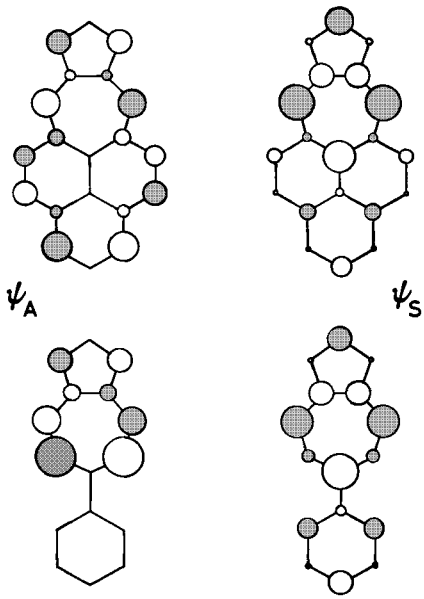

Fig. 5. *The two lowest antibonding HMO's* (ψ_S and ψ_A) *of azuleno*[*5.6.7*-cd]*phenalene* (I) *and 6-phenylazulene* (II). The radii of the circles are proportional to the absolute values of the LCAO coefficients. Blank and dotted areas symbolize different signs

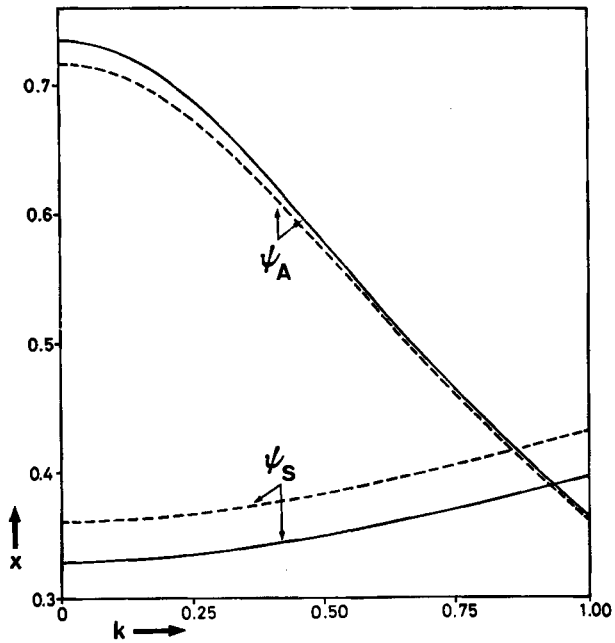

Fig. 6. *HMO energies* $E = \alpha + x\beta$ *of azuleno*[*5.6.7*-cd]*phenalene* (I) vs. *the parameter* $\beta_{\mu\nu} = k\beta$ *of the bonds 4a–5, 6–6a, 9a–10 and 11–11a.* The parameter $\beta_{\mu\nu}$ of the 3a–12a bond set equal to β (——) or 0.8 β (– – – –)

and its derivatives (dashed lines) [5]. Evidently, a value of k smaller than these numbers should be adopted for an HMO model of I, in order to produce the correct energy sequence (ψ_S *below* ψ_A). Such a value of k would also be consistent with the low order predicted for the four bonds [4]: $p_{\mu\nu} = 0.443$ (4a–5 and 11–11a) and 0.432 (6–6a and 9a–10).

Table. *Proton coupling constants* (a_{H_μ} in gauss $= 10^{-4}$ tesla) *and calculated π-spin populations* (ϱ_μ) *for the radical anions* $I^\ominus$, *I-*$d_2^\ominus$, $II^\ominus$, *II-*$d_2^\ominus$ *and* $III^\ominus$

	$I^\ominus$, I-$d_2^\ominus$			$II^\ominus$, II-$d_2^\ominus$		$III^\ominus$	
μ [a]	$a_{H\mu}$ [b]	ρ_μ [c]	μ [d]	$a_{H\mu}$ [b]	ρ_μ [e]	$a_{H\mu}$ [f]	ρ_μ [e]
1,3	0.27[g]	-0.024	1,3	0.35[g]	-0.029	0.28	-0.029
2	4.19	0.131	2	3.85	0.112	3.98	0.131
4,12	5.04	0.252	4,8	4.90	0.196	6.22	0.280
5,11	0.88	0.034					
6,10	0.31[h]	-0.028					
7,9	0.73[h]	-0.026	3',5'	0.70[h]	-0.028		
8	2.52	0.068	4'	2.08	0.098		
13	-	0.176	6	-	0.258	8.87	0.360
14	-	-0.011	1'	-	-0.006		
3a,12a	-	0.086	3a,8a	-	0.079	-	0.079
4a,11a	-	-0.032	5,7	0.75[h]	-0.034	1.27	-0.076
6a,9a	-	0.056	2',6'	1.75	0.086		

[a] Numbering of the positions μ in azuleno[5.6.7-*cd*]phenalene (*cf.* formula I).
[b] Experimental error: ± 0.02 and ± 0.01 gauss for $a_{H\mu}$ larger and smaller than 1 gauss, respectively.
[c] Calculated with $\beta_{\mu\nu} = 0{,}8\beta$ for the bonds 3a–12a, 4a–5, 6–6a, 9a–10 and 11–11a, and with $\lambda = 1.2$ (cf. text).
[d] Numbering of the positions μ in azulene and 6-phenylazulene (*cf.* formula II).
[e] Calculated with $\beta_{\mu\nu} = 0.8\beta$ for the bond 3a–8a, and with $\lambda = 1.2$ (*cf.* text).
[f] Taken from ref. [8].
[g] Replaced by unresolved deuteron splitting for I-$d_2^\ominus$ and II-$d_2^\ominus$: $0.1535\, a_{H_{1,3}} = a_{D_{1,3}} (< 0.06)$.
[h] Assignment uncertain.

The π-spin populations ϱ_μ listed in the Table were calculated according to the *McLachlan* procedure [9] with the conventional value $\lambda = 1.2$. The parameter $\beta_{\mu\nu} = 0.8\beta$ was used for the long bond 3a–8a in II and III, as well as for the analogous bond 3a–12a in I. The same value of $\beta_{\mu\nu}$, *i.e.* $k = 0.8$ in the diagram of Figure 6, also served for the four relevant bonds in I considered above. Proportionality $a_{H\mu} = Q \cdot \varrho_\mu$ between the observed proton coupling constants $a_{H\mu}$ and the calculated π-spin populations ϱ_μ is only fair. The rather poor constancy of Q in the case of azulene

radical anion ($III^{\ominus}$) has been noticed by previous workers [6]. This unsatisfactory feature seems thus to be shared not only by the radical anion of the 6-phenylderivative ($II^{\ominus}$), but also by that of the structurally related azuleno[5.6.7-*cd*]phenalene ($I^{\ominus}$).

It is tempting to use the HMO model of I for an estimation of the energy gap between the orbitals ψ_S and ψ_A. The diagram of Figure 6 suggests a value less than $0.1|\beta| \approx 0.25$ eV if the number k is not decreased below 0.75. Such a small energy gap might result in a triplet ground state of the dianion $I^{2\ominus}$. However, although this dianion is readily formed, its glassy solution in MTHF fails to display ESR. signals characteristic of the triplet state (*cf.* Experimental Part). It must therefore be concluded that $I^{2\ominus}$ has a singlet ground state and that more sophisticated MO methods are required to rationalize this finding in terms of orbital energies.

Support by the *Schweizerischer Nationalfonds zur Förderung der wissenschaftlichen Forschung* (Project Nr. 2.824.73) is acknowledged.

REFERENCES

[1] *F. Gerson*, «Hochauflösende ESR.-Spektroskopie dargestellt anhand aromatischer Radikal-Ionen», Verlag-Chemie, Weinheim, 1967; English Edition: 'High Resolution ESR Spectroscopy', Verlag-Chemie, Weinheim, and J. Wiley & Sons, New York, 1970.
[2] *Ch. Jutz, R. Kirchlechner & H.-J. Seidel*, Chem. Ber. *102*, 2301 (1969).
[3] *E. D. Bergmann & R. Ikan*, J. Amer. chem. Soc. *78*, 482 (1955); *H. Pommer*, Archiv. Pharm. *291/63*, 23 (1958); *Ch. Jutz et al.*, Chem. Ber., in press.
[4] *H. Fischer & G. Ege*, Chem. Ber. *100*, 395 (1967).
[5] *E. Heilbronner*, in 'Non-Benzenoid Aromatic Compounds' (D. Ginsburg, ed.). J. Wiley & Sons (Interscience), New York, 1959; pp. 171–276.
[6] *I. Bernal, P. H. Rieger & G. K. Fraenkel*, J. chem. Physics *37*, 1489 (1962).
[7] *A. H. Reddoch*, J. chem. Physics *43*, 225 (1965).
[8] *F. Gerson, J. Heinzer & E. Vogel*, Helv. *53*, 95 (1970).
[9] *A. D. McLachlan*, Mol. Physics *3*, 233 (1960).

---

156. Comparison of ^{13}C- and ^{1}H-Magnetic Resonance Spectroscopy as Techniques for the Quantitative Investigation of Dynamic Processes. The Cope Rearrangement in Bullvalene

by **Jean F. M. Oth, Klaus Müllen, Jean-Marie Gilles** and **Gerhard Schröder**

Laboratory for organic chemistry, E.T.H., CH–8006 Zürich
Institute for organic chemistry, University of Karlsruhe, D–7500 Karlsruhe

(15. V. 74)

Summary. The potential advantages of ^{13}C-(^{1}H-noise decoupled) spectroscopy (in the *Fourier* transform mode) over ^{1}H-spectroscopy for the quantitative investigation of molecular dynamic processes is discussed. The *Cope* rearrangement in bullvalene, an example of complex exchange of spins over different magnetic sites, has been studied by both kinds of spectroscopy as a test.

1. Introduction. – Temperature dependent NMR. spectra of molecules undergoing fast dynamic processes can in principle be quantitatively analysed and the kinetic data characteristic of the dynamics thus be obtained. The required line shape